Studying the squeezing effect and phase-space distribution of a single-photon-added coherent state using a postselected von Neumann measurement

Wen Jun Xu, Taximaiti Yusufu, and Yusuf Turek ●*

School of Physics and Electronic Engineering, Xinjiang Normal University, Urumqi, Xinjiang 830054, China

In this paper, ordinary and amplitude-squared squeezing as well as Wigner functions of single-photon-added coherent state after postselected von Neumann measurements are investigated. The analytical results show that the weak measurement procedure, which is characterized by postselection and weak value, can significantly change the principal squeezing feature of the single-photon-added coherent state. From the analysis of the Winger function we notice that in the strong measurement regime significant interference structures manifest and the negative regions become larger than the initial pointer state. Our results indicate that after postselected von Neumann measurement the degree of nonclassicality of single-photon-added coherent state is increased. It is anticipated that this work may provide alternate and effective methods for solving the state optimization problems based on the single-photon-added coherent state pointer via a postselected von Neumann measurement technique.

I. INTRODUCTION

States which possess nonclassical features are an important resource for quantum information processing and the investigation of fundamental problems in quantum theory. It was shown that squeezed states of radiation fields can be considered truly quantum [1]. In recent years, studies concerning squeezing, especially quadrature squeezing of radiation fields, have received considerable attention as squeezing may have applications in optical communication and information theory [2–13], gravitational wave detection [14], quantum teleportation [14–22], dense coding [23], resonance fluorscence [24], and quantum cryptography [25]. Furthermore, with the rapid development of the techniques for making higher-order correlation measurements in quantum optics and laser physics, the higher-order squeezing effects of radiation fields have also became a hot topic in state optimization research. Higher-order squeezing of radiation fields was first introduced by Hong and Mandel [26] in 1985. Hilley [27,28] defined another type of higher-order squeezing, named amplitude-squared (AS) squeezing, of the electromagnetic field in 1987. Following this work, the higher-order squeezing of radiation fields has been investigated across many fields of research [29–45].

Squeezing is an inherent feature of nonclassical states and its improvement requires optimization. Some states do not initially possess squeezing, but after undergoing an optimization process they may possess a pronounced squeezing effect. The single-photon-added coherent (SPAC) state is a typical example [46,47]. SPAC states are created by adding the creation operator $a^{\dagger}$ to the coherent state. This optimization changes the coherent state from semi-classical to a new quantum state which possess squeezing [48]. Since this state has wide applications across many quantum information processes, including quantum communication [49], quantum key distribution [50–53], and quantum digital signature [54], the optimization for this state is worthy of study. In particular, it may provide another method to the implementations of the related processes. However, the weak signal amplification technique proposed in 1988 [55] by Aharonov, Albert, and Vaidman was widely used in state optimization and precision measurement problems [56–62]. Most recently, one of the authors of this paper investigated the effects of postselected von Neumann measurement on the properties of single-mode radiation fields [61,62] and found that it can change the photon statistics and quadrature squeezing of radiation fields for different anomalous weak values and coupling strengths. In previous works, squeezing strongly depended on the phases of the field quadrature components and it needed to be modified if we regarded its detection process. However, there is another type of definition of squeezing named principal squeezing [63]. Principal squeezing is a rotational invariant and is independent of the phase of the local oscillator. It can occur more frequently than the standard squeezing we generally use. Most interestingly, principal squeezing is really measured in the homodyne detection, supposing the quadrature correlation to be different from zero for a value of the local oscillator phase [63]. Here we have to mention that in our previous work [62], we only considered the ordinary squeezing with the standard squeezing definition [64]. Furthermore, if we regarded the squeezing detection process, the ordinary and higher-order squeezing needed a new kind of squeezing definition. But, to the best of our knowledge, the effects of postselected von Neumann measurement on ordinary and higher-order principal squeezing of radiation fields has not been previously investigated.

In this work, motivated by our prior works [59,61,62], we study the principal squeezing and phase-space

---

edistribution characterized by the Winger function of the SPAC state after postselected von Neumann measurement. In this study, we take the spatial and polarization degrees of freedom of the SPAC state as a pointer (measuring device) and system (measured system), respectively, and consider all orders of the time evolution operator. Following the determination of the final state of the pointer, we check the criteria for the existence of the principal squeezing of the SPAC state and find that the postselected measurement has positive effects on squeezing of the SPAC state in the weak measurement region. Furthermore, we investigate the state-distance and the Wigner function of the SPAC state after measurement. We find that, by increasing the coupling strength, the original SPAC state spoils significantly, and the state exhibits more pronounced negative areas as well as interference structures in phase space after the postselected measurement. We observe that the postselected von Neumann measurement has positive effects on its nonclassicality, including squeezing effects, especially in the weak measurement region. Since the improvements of those effects caused by the anomalous weak values are in the weak measurement procedure, they can be considered a result of the weak value amplification of the weak measurement technique.

This paper is organized as follows. In Sec. II, we introduce the main concepts of our scheme and derive the final pointer state after the postselected measurement, which will be used throughout the study. In Sec. III, we give details of the ordinary squeezing and AS squeezing effects of the final pointer state by using the principal squeezing definition. In Sec. IV, we investigate the state distance and the Wigner function SPAC state after measurement. A conclusion is given in Sec. V.

II. MODEL AND THEORY

In this section, we introduce the basic concepts of postselected von Neumann measurement and give the expression of the final pointer state which we use in this paper. We know that every measurement problem consists of three main parts, including a pointer (measuring device), measured system, and the environment. In the current work, we take the spatial and polarization degrees of freedom of the SPAC state as the pointer and system, respectively. In general, in measurement problems, we want to determine the system information of interest by comparing the state shifts of the pointer after the measurement finishes, thus we do not consider the spoiling of the pointer in the entire measurement process. Here, contrary to the standard goal of the measurement, we investigate the effects of pre and postselected measurements taken on a beam's polarization (measured system) on the inherent properties of a beam's spatial component (pointer). In the measurement process, the system and pointer Hamiltonians do not effect the final readouts, so it is sufficient to only consider their interaction Hamiltonian for our purposes. According to standard von Neumann measurement theory [65], the interaction Hamiltonian between the system and the pointer takes the form

$$\hat{H} = g(t)\hat{A} \otimes \hat{P}. \qquad (1)$$

Here $\hat{A}$ is the system observable we want to measure and $\hat{P}$ is the momentum operator of the pointer conjugated with

the position operator $[\hat{X}, \hat{P}] = i$. $g(t)$ is the coupling strength function between the system and pointer, and it is assumed exponentially small except during a period of interaction time of order T. The coupling strength function $g(t)$ is normalized according to $\int_{-\infty}^{+\infty} g(t)dt = \int_0^T g(t)dt = g_0$. In the current work, we assume that the system observable A is the Pauli x matrix, i.e.,

$$\hat{A} = \hat{\sigma}_x = |H\rangle\langle V| + |V\rangle\langle H| = \begin{pmatrix} 0 & 1 \\ 1 & 0 \end{pmatrix}. \qquad (2)$$

Here $|H\rangle \equiv (1, 0)^T$ and $|V\rangle \equiv (0, 1)^T$ represent the horizontal and vertical polarizations of the beam, respectively. We also assume that, in our scheme, the pointer and measurement system are initially prepared to

$$|\phi\rangle = \gamma a^\dagger|\alpha\rangle, \quad \gamma = \frac{1}{\sqrt{1 + |\alpha|^2}}, \qquad (3)$$

and

$$|\psi_i\rangle = \cos\frac{\varphi}{2}|H\rangle + e^{i\delta}\sin\frac{\varphi}{2}|V\rangle, \qquad (4)$$

respectively. Here $\alpha = re^{i\theta}$ and $\delta \in [0, 2\pi]$ and $\varphi \in [0, \pi)$. The SPAC state can represent the result of successive elementary one-photon excitation of a classical coherent field and occupy an intermediate position between the single photon and the coherent states, reducing to the two-limit cases for $|\alpha| \to 0$ or $|\alpha|$ being larger than 1, respectively [48].

Here we are reminded that, in weak measurement theory, the interaction strength between the system and measurement is weak. Hence it is enough to only consider the evolution of the unitary operator up to its first order. However, if we want to connect the weak and strong measurements and investigate the measurement feedback of postselected weak measurement procedures and analyze the experimental results obtained in nonideal measurements, the full-order evolution of the unitary operator is needed [66–68], We call this kind of measurement a postselected von Neumann measurement. Thus, the evolution operator of this total system corresponding to the interaction Hamiltonian, Eq. (1), is evaluated as

$$e^{-ig_0\hat{\sigma}_x\otimes\hat{P}} = \frac{1}{2}(\hat{I} + \hat{\sigma}_x) \otimes D\left(\frac{s}{2}\right) + \frac{1}{2}(\hat{I} - \hat{\sigma}_x) \otimes D\left(-\frac{s}{2}\right), \quad (5)$$

since $\hat{\sigma}_x^2 = 1$. Here $s = \frac{g_0}{\sigma}$ is the ratio between the coupling strength and beam width and it can characterize the measurement types, i.e., the measurement is considered a weak measurement (strong measurement) if $s < 1$ ($s > 1$). $D(\frac{s}{2})$ is the displacement operator defined as $D(\alpha) = e^{\alpha\hat{a}^\dagger - \alpha^*\hat{a}}$. The results of our current research are valid for weak and strong measurement regimes since we take into account the all orders of the time evolution operator, Eq. (5). In the above calculation we use the definition of the position and momentum operator represented in Fock space in terms of an annihilation (creation) operator $\hat{a}$ ($\hat{a}^\dagger$), i.e.,

$$\hat{X} = \sigma(\hat{a}^\dagger + \hat{a}), \qquad (6)$$

$$\hat{P} = \frac{i}{2\sigma}(a^\dagger - a), \qquad (7)$$

where σ is considered as the size of ground-state wave packet of the beam. Thus, the total state of the system $|\psi_i\rangle \otimes |\phi\rangle$ after

the time evolution changes to

$$
\begin{aligned}
|\Psi\rangle &= e^{-ig_0\hat{\sigma}_x\otimes\hat{P}}|\psi_i\rangle\otimes|\phi\rangle \\
&= \frac{1}{2}\left[(\hat{I}+\hat{\sigma}_x)\otimes D\left(\frac{s}{2}\right)+(\hat{I}-\hat{\sigma}_x)\otimes D\left(\frac{-s}{2}\right)\right]|\psi_i\rangle \\
&\quad \otimes|\phi\rangle.
\end{aligned} \tag{8}
$$

After we take a strong projective measurement onto the polarization degree of the beam with postselected state $|\psi_f\rangle=|H\rangle$, the above total system state gives us the final state of the pointer and its normalized expression reads as

$$
|\Phi\rangle = \frac{\kappa}{\sqrt{2}}\left[(1+\langle\sigma_x\rangle_w)D\left(\frac{s}{2}\right)+(1-\langle\sigma_x\rangle_w)D\left(-\frac{s}{2}\right)\right]|\phi\rangle. \tag{9}
$$

Here

$$
\begin{aligned}
\kappa^{-2} &= 1+|\langle\sigma_x\rangle|^2+\gamma^2 e^{-\frac{s^2}{2}}\mathrm{Re}[(1+\langle\sigma_x\rangle_w^*)(1-\langle\sigma_x\rangle_w) \\
&\quad\times(\gamma^{-2}-s^2+\alpha s-\alpha^* s)e^{2si\mathrm{Im}[\alpha]}]
\end{aligned} \tag{10}
$$

is the normalization coefficient and the weak value of the system observable $\hat{\sigma}_x$ is given by

$$
\langle\hat{\sigma}_x\rangle_w = \frac{\langle\psi_f|\sigma_x|\psi_i\rangle}{\langle\psi_f|\psi_i\rangle} = e^{i\delta}\tan\frac{\varphi}{2}. \tag{11}
$$

In general, the expectation value of $\hat{\sigma}_x$ is bounded $-1\leqslant\langle\hat{\sigma}_x\rangle_{\mathrm{ex}}\leqslant 1$ for any associated system state. However, as we can see in Eq. (11), the weak values of the observable $\hat{\sigma}_x$ can take arbitrary large numbers with small successful postselection probability $P_s=|\langle\psi_f|\psi_i\rangle|^2=\cos^2\frac{\varphi}{2}$. This weak value feature is used to amplify very weak but useful information on various forms of the related physical systems [69–77]. For details of the applications of weak measurement in signal amplification processes, we refer the reader to the recent overview of the field [78,79].

The state given in Eq. (9) is a spoiled version of the SPAC state after postselected measurement. In the next sections, we study the squeezing effects and the phase-space distribution, namely the Wigner function of the state $|\Phi\rangle$.

III. ORDINARY AND AMPLITUDE SQUARE SQUEEZING

In this section, we check the ordinary (first-order) and AS (second-order) squeezing effects of the SPAC state after postselected von Neumann measurement. The squeezing effect is

one of the nonclassical phenomena unique to the quantum light field. The squeezing reflects the nonclassical statistical properties of the optical field by a noise component lower than that of the coherent state. In other words, the noise of an orthogonal component of the squeezed light is lower than the noise of the corresponding component of the coherent-state light field. In practice, if this component is used to transmit information, a higher signal-to-noise ratio can be obtained than that of the coherent state. Consider a single mode of electromagnetic field of frequency ω with creation and annihilation operators $a^\dagger, a$. The quadrature and square of the field-mode amplitude can be defined by operators X_ϑ and Y_ϑ as [64]

$$
X_\vartheta \equiv \tfrac{1}{2}(ae^{-i\vartheta}+a^\dagger e^{i\vartheta}), \tag{12}
$$

and

$$
Y_\vartheta \equiv \tfrac{1}{2}(a^2 e^{-i\vartheta}+a^{\dagger 2}e^{i\vartheta}), \tag{13}
$$

respectively. For these operators, if $\triangle X_\vartheta\equiv X_\vartheta-\langle X_\vartheta\rangle$, $\triangle Y_\vartheta\equiv Y_\vartheta-\langle Y_\vartheta\rangle$, the minimum variances with respect to all the possible phases ϑ are [63,80]

$$
\langle(\triangle X_\vartheta)^2\rangle_{\min} = \tfrac{1}{4}+\tfrac{1}{2}[(\langle a^\dagger a\rangle-|\langle a\rangle|^2)-|\langle a^2\rangle-\langle a\rangle^2|], \tag{14}
$$

and

$$
\begin{aligned}
\langle(\triangle Y_\vartheta)^2\rangle_{\min} &= \langle a^\dagger a+\tfrac{1}{2}\rangle+\tfrac{1}{2}[\langle a^{\dagger 2}a^2\rangle-|\langle a^2\rangle|^2 \\
&\quad -|\langle a^4\rangle-\langle a^2\rangle^2|],
\end{aligned} \tag{15}
$$

respectively. Here a and $a^\dagger$ are annihilation and creation operators of the radiation field. If $\langle(\triangle X_\vartheta)^2\rangle_{\min}<\frac{1}{4}$, X_ϑ is said to be ordinary squeezeing and if $\langle(\triangle Y_\vartheta)^2\rangle_{\min}<\langle a^\dagger a+\frac{1}{2}\rangle$, Y_ϑ is said to be AS squeezing. These conditions can be rewritten as

$$
S_{\mathrm{os}} = \langle a^\dagger a\rangle-|\langle a\rangle|^2-|\langle a^2\rangle-\langle a\rangle^2|<0, \tag{16}
$$

and

$$
S_{\mathrm{ass}} = \langle a^{\dagger 2}a^2\rangle-|\langle a^2\rangle|^2-|\langle a^4\rangle-\langle a^2\rangle^2|<0. \tag{17}
$$

Thus, the system characterized by any wave function may exhibit nonclassical features if it satisfies Eqs. (16) and (17).

The above criteria for the existince of squeezing is a result of the principal squeezing [63].

To achieve our goal, we first have to calculate the above related quantities under the state $|\Phi\rangle$. After some calculations we can get their explicit expressions. Those are listed below.

(1) The expectation value $\langle a^\dagger a\rangle$ under the state $|\Phi\rangle$ is given by

$$
\langle a^\dagger a\rangle = |\kappa|^2\{|1+\langle\sigma_x\rangle_w|^2 t_1(s)+|1-\langle\sigma_x\rangle_w|^2 t_1(-s)+2\mathrm{Re}[(1-\langle\sigma_x\rangle_w)(1+\langle\sigma_x\rangle_w)^* t_2(s)]\}, \tag{18}
$$

where

$$
t_1(s) = \gamma^2((2+|\alpha|^4+s|\alpha|^2)\mathrm{Re}(\alpha)+3\alpha\alpha^*+1)+\frac{s^2}{4},
$$

and

$$
\begin{aligned}
t_2(s) &= \tfrac{1}{4}\gamma^2 e^{2is\mathrm{Im}(\alpha)}e^{-\frac{s^2}{2}}\{4|\alpha|^4-6s\alpha|\alpha|^2+2[6\alpha\alpha^*+s\alpha^{*2}(3\alpha+s) \\
&\quad +s\mathrm{Re}(\alpha)(8-9s\alpha-3s^2)]+11\alpha^2 s^2+s^4+6\alpha s^3-5s^2-16\alpha s+4\},
\end{aligned}
$$

respectively.

(2) The expectation value $\langle \hat{a} \rangle$ under the state $|\Phi\rangle$ is given by

$$\langle \hat{a} \rangle = |\kappa|^2 \gamma^2 \left\{ |1 + \langle \sigma_x \rangle_w|^2 \left(2\alpha + \alpha|\alpha|^2 + \frac{s}{2\gamma^2} \right) + |1 - \langle \sigma_x \rangle_w|^2 \left(2\alpha + \alpha|\alpha|^2 - \frac{s}{2\gamma^2} \right) \right.$$
$$\left. + (1 - \langle \sigma_x \rangle_w)(1 + \langle \sigma_x \rangle_w)^* w_1(-s) + (1 + \langle \sigma_x \rangle_w)(1 - \langle \sigma_x \rangle_w)^* w_1(s) \right\}, \quad (19)$$

where

$$w_1(s) = \tfrac{1}{2} e^{-2si\mathrm{Im}(\alpha)} [2\alpha(2 + |\alpha|^2) + 3s\gamma^{-2} - 2\alpha^2 s + s^2(\alpha^* - 3\alpha)] e^{-\frac{s^2}{2}}.$$

(3) The expectation value $\langle \hat{a}^2 \rangle$ under the state $|\Phi\rangle$ is given by

$$\langle \hat{a}^2 \rangle = |\kappa|^2 \{ |1 + \langle \sigma_x \rangle_w|^2 q_1(s) + |1 - \langle \sigma_x \rangle_w|^2 q_1(-s) + (1 - \langle \sigma_x \rangle_w)(1 + \langle \sigma_x \rangle_w)^* q_2(s) + (1 + \langle \sigma_x \rangle_w)(1 - \langle \sigma_x \rangle_w)^* q_2(-s) \}, \quad (20)$$

where

$$q_1(s) = \tfrac{1}{4} \gamma^2 (2\alpha + s)[6\alpha + |\alpha|^2(2\alpha + s) + s],$$

and

$$q_2(s) = -\tfrac{1}{4} e^{2is\mathrm{Im}(\alpha)} e^{-\frac{s^2}{2}} \gamma^2 (s - 2\alpha)[6\alpha + \alpha^*(s - 2\alpha)(s - \alpha) + 2\alpha^2 s + s^3 - 3\alpha s^2 - 5s],$$

respectively.

(4) The expectation value $\langle \hat{a}^{\dagger 2} \hat{a}^2 \rangle$ under the state $|\Phi\rangle$ is given by

$$\langle \hat{a}^{\dagger 2} \hat{a}^2 \rangle = |\kappa|^2 \{ |1 + \langle \sigma_x \rangle_w|^2 f_1(s) + |1 - \langle \sigma_x \rangle_w|^2 f_1(-s) + 2\mathrm{Re}[(1 - \langle \sigma_x \rangle_w)(1 + \langle \sigma_x \rangle_w)^* f_2(s)] \}, \quad (21)$$

where

$$f_1(s) = \frac{1}{2} \gamma^2 \{ 2|\alpha|^6 + s|\alpha|^2 [(s^2 + 16)\mathrm{Re}(\alpha) + s\mathrm{Re}(\alpha^2)] + 2|\alpha|^4 [2s\mathrm{Re}(\alpha) + s^2 + 5]$$
$$+ 8\alpha^* \alpha + 6s^2 \alpha^* \alpha + (2s^3 + 8s)\mathrm{Re}(\alpha) + 3s^2 Re(\alpha^2) \} + \frac{s^4}{16} + \gamma^2 s^2,$$

and

$$f_2(s) = -\frac{1}{16} \gamma^2 (s - 2\alpha)(2\alpha^* + s) \left(2(\alpha^*)^2(s - 2\alpha)(s - \alpha) + 20|\alpha|^2 + 3s\alpha^*(s - 2\alpha)(s - \alpha) \right.$$
$$\left. + 28is\mathrm{Im}(\alpha) + s^2(2\alpha^2 + s^2 - 3\alpha s - 9) + 16 e^{-\frac{1}{2}s(s - 4i\mathrm{Im}[\alpha])} \right),$$

respectively.

(5) The expectation value $\langle \hat{a}^4 \rangle$ under the state $|\Phi\rangle$ is given by

$$\langle \hat{a}^4 \rangle = |\kappa|^2 \{ |1 + \langle \sigma_x \rangle_w|^2 h_1(s) + |1 - \langle \sigma_x \rangle_w|^2 h_1(-s) + (1 + \langle \sigma_x \rangle_w)^*(1 - \langle \sigma_x \rangle_w) h_2(s)$$
$$+ (1 + \langle \sigma_x \rangle_w)(1 - \langle \sigma_x \rangle_w)^* h_2(-s) \}, \quad (22)$$

where

$$h_1(s) = \tfrac{1}{16} [8\alpha \gamma^2 |\alpha|^2 (\alpha + s)(2\alpha^2 + s^2 + 2\alpha s) + s^4 + 8\alpha \gamma^2 (10\alpha^3 + 2s^3 + 9\alpha s^2 + 16\alpha^2 s)],$$

and

$$h_2(s) = -\tfrac{1}{16} \gamma^2 e^{2is\mathrm{Im}(\alpha)} e^{-\frac{s^2}{2}} (s - 2\alpha)^3 [10\alpha + \alpha^*(s - 2\alpha)(s - \alpha) + 2\alpha^2 s + s^3 - 3\alpha s^2 - 9s],$$

respectively.

Here we have to mention that, if $\langle a^2 \rangle - \langle a \rangle^2$ and $\langle \langle a^4 \rangle - \langle a^2 \rangle^2 \rangle$ are all real, respectively, then the principal squeezing and standard squeezing which we used in previous work [62] are equivalent [63]. However, in this work, as we can see, those quantities both are complex and it give a rotationally invariant squeezing effect in contrast to the prior work.

Using the expression for S_{os}, the curves for this quantity are plotted and the analytical results are shown in Fig. 1. In Fig. 1(a), we fix the parameter $r = 1$ and plot S_{os} as a function of the coupling factor s for different weak values quantified by φ. As we observe, when there is no interaction between the system and the pointer ($s = 0$), there is no ordinary squeezing effect of the initial SPAC state. However, in the moderate coupling factor regions such as $0 < s < 2$, the ordinary squeezing effect of the SPAC state is proportional to the weak value, i.e., the larger the weak value, the better its squeezing effect. From Fig. 1(a) we also can see that the ordinary squeezing effect of the light field gradually disappears and tends to the same value for different weak values by increasing the coupling factor s in the strong measurement regime. In Fig. 1(b), we plot S_{os} as a function of the state parameter r in the weak measurement regime by fixing the coupling factor s ($s = 0.5$).
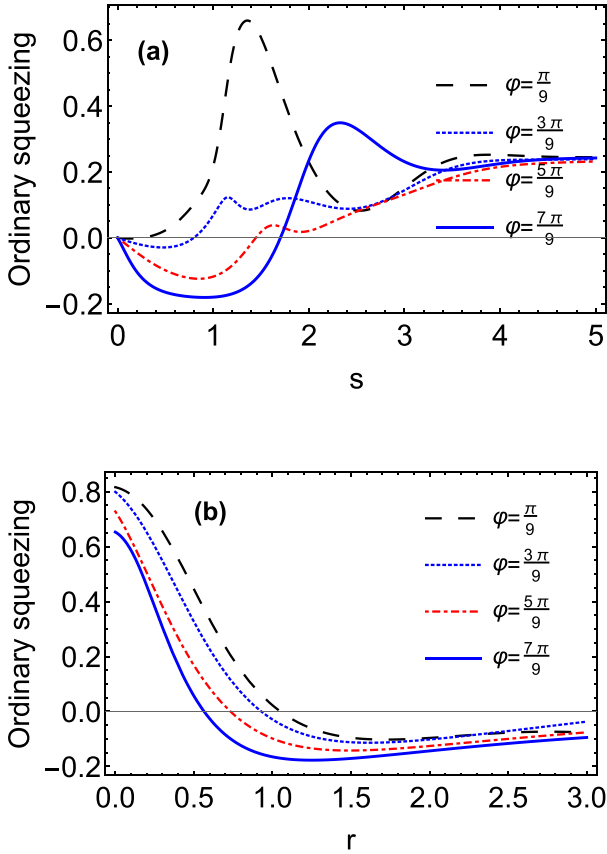
FIG. 1. The effects of postselected von Neumann measurement on ordinary squeezing of SPAC state. Panel (a) shows the quantity S_{os} as a function of coupling factor for different weak values with fixed coherent state parameter ($r = 1$). Panel (b) shows quantity S_{os} as a function of coherent state parameter r for different weak values with fixed coupling factor ($s = 0.5$). Here we take $\theta = \frac{\pi}{4}$, $\delta = \frac{\pi}{6}$.

FIG. 2. The effects of postselected von Neumann measurement on AS squeezing of SPAC state. (a) the S_{ass} as a function of coupling factor s for different weak values with fixed coherent state parameter r ($r = 1$); (b) the S_{ass} as a function of coherent state parameter r for different weak values with fixed weak coupling factor s ($s = 0.5$). Other parameters are the same as those used in Fig. 1.

It is very clear from the curves presented in Fig. 1(b) that the ordinary squeezing effect of the SPAC state is increased when increasing the weak value, especially when φ is taken as $\frac{7\pi}{9}$. Furthermore, along with the increasing r (for r values exceeding 1.5), the squeezing effect of the field for different weak values tends to be the same. In the weak measurement procedure the SPAC state shows a good ordinary squeezing effect after postselected measurement with large weak values. This can be seen as a result of the signal amplification feature of the weak measurement technique.

The quantity S_{ass} can characterize the AS squeezing of the SPAC state if it takes negative values. In Fig. 2 it is plotted as a function of various system parameters. As indicated in Fig. 2(a), when we fix the coherent state parameter r, the S_{ass} can take negative values in the weak measurement regime ($s < 1$); its negativity increases when increasing the weak value quantified by φ. That is to say, in the weak measurement procedure, the magnitude of the weak value has a linear relationship with the AS squeezing effect of the SPAC state, i.e., the larger the weak value, the better the AS squeezing effect. However, by increasing the coupling strength, the value of S_{ass} becomes larger than zero and it indicates that there is no AS squeezing effect of the SPAC state in the postselected strong measurement regime ($s > 1$) no matter how large the weak

value is taken to be. To further investigate the AS squeezing of the radiation field in the weak measurement procedure, we plot S_{ass} as a function of the coherent state parameter r for different weak values with fixed coupling factor ($s = 0.5$). The analytical results are shown in Fig. 2(b). We can see that when r is relatively small, there is no AS squeezing effect no matter how large the weak value we take. By increasing the system parameter r, S_{ass} takes negative values and its negativity is proportional to r. From Fig. 2(b) we can also observe that, in the weak measurement procedure, the weak values have positive effects on the AS squeezing of the SPAC state and it can also be considered a result of the weak signal amplification feature of the postselected weak measurement technique.

According to the results of recent theoretical and experimental studies [81,82], when the interaction strength changed from weak to strong postselected measurement regimes, the value of the system observable changed from weak value to the expectation value, respectively, and there was not any signal amplification effect in strong measurement regimes. Thus, in strong postselected von Neumann measurement the "weak value" has no significant impact on the inherent properties of

the system. This statement can also be verified in Figs. 1(a) and 2(a).

IV. STATE DISTANCE, MEASUREMENT ACCURACY, AND WIGNER FUNCTION

A. State distance

The postselected measurement taken on the polarization degree of freedom of the beam could spoil the inherent properties presented in its spatial part. Before we investigate the phase-space distribution of the SPAC state after postselected von Neumann measurement, we check the similarity between the initial SPAC state $|\phi\rangle$ and the state $|\Phi\rangle$ after measurement. The state distance between these two states can be evaluated by

$$F = |\langle\phi|\Phi\rangle|^2, \tag{23}$$

and its value is bounded $0 \leqslant F \leqslant 1$. If $F = 1$ ($F = 0$), then the two states are totally the same (totally different). The F in our case can be calculated after substituting Eqs. (3) and (9) into Eq. (23) and the analytical results are shown in Fig. 3. In Fig. 3(a) we present the state distance F as a function of state parameter r for different coupling factors with a fixed, large weak value. As shown in Fig. 3(a), in the weak coupling regime ($s = 0.5$), the state after the postselected measurement maintains its similarity with the initial pointer state $|\phi\rangle$ as the coherent state parameter r increases. However, by increasing the coupling factor, the initial state $|\phi\rangle$ is spoiled and the similarity between the pointer states before and after the measurement decreases dramatically [see Figs. 3(a) and 3(b)]. Furthermore, from Fig. 3(b) we can observe that the distortion of the SPAC state after the measurement strongly relates to the magnitude of weak values and coupling factors. In the weak measurement regime ($0 < s < 1$), the larger the anomalous weak value is, the larger the distortion of the state occurrs.

In contrast to the original purpose of the weak value achieved in the two-state vector formalism of quantum theory [55], the role of the weak value in the present work is to manipulate the external degrees of freedom of the pointer state rather than to obtain information of the system. In general, there are three kinds of existing values of a system observable including the eigenvalue, expectation value, and weak value, which depends on different measurement circumstances. Among them, the eigenvalue and expectation value usually occurr in strong measurement models, but the weak value is a natural way to express the value of the system observable in pre and postselected intervals in the weak measurement procedure. The transition from the weak value to the (conditional) expectation value can be realized by making the transition from Aharonov's weak measurement to von Neumann's strong measurement. This transition is characterized by a transition factor $e^{-s^2/2}$ [81,82]. However, the actual effects of those three values on the pointer is not very clear, but a recent study [83] gave a clue to this puzzle. The authors investigated the fact that the nature of the weak value is different from the nature of the expectation value of the system observable, so the weak value describes the interaction in the same way as the eigenvalue does.
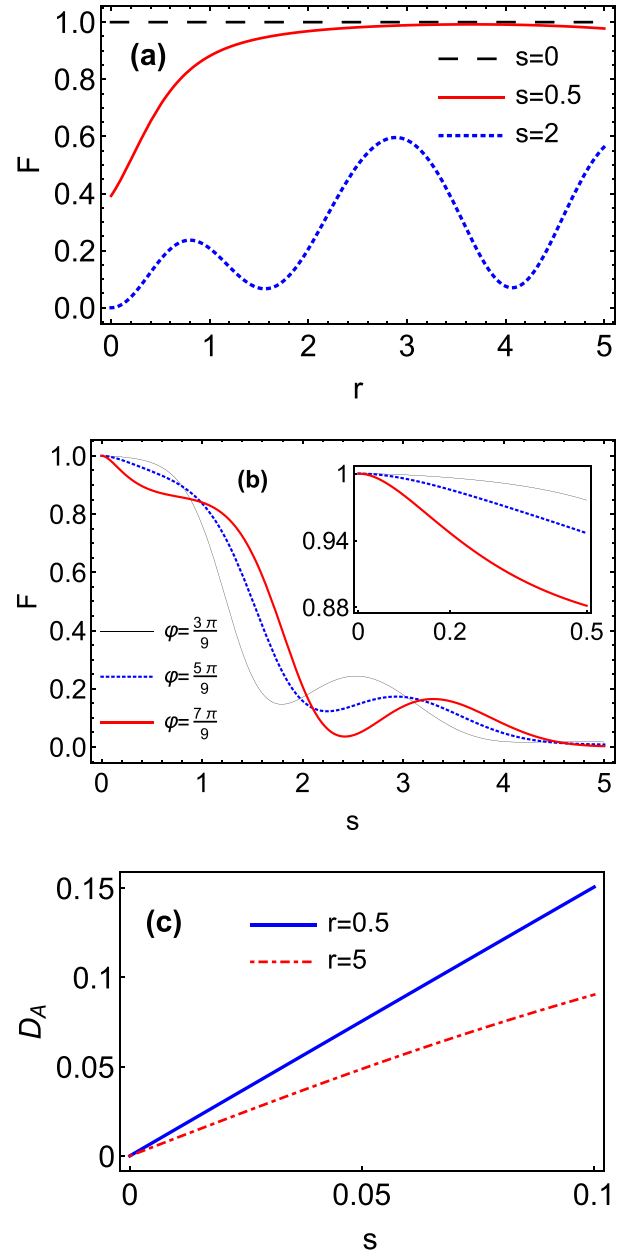
FIG. 3. The state distortion after taking measurement. (a) The state distance between $|\Phi\rangle$ and initial SPAC state $|\phi\rangle$ as a function of coherent state parameter r for various coupling factors. (b) The state distance between $|\Phi\rangle$ and initial SPAC state $|\phi\rangle$ as a function of coupling factor s for various weak values, and we $r = 1$. (c) The Bures angle, Eq. (24), as a function of coupling factor s for various coherent state parameter r. Here, we set other parameter as $\theta = \frac{\pi}{4}$, $\delta = \frac{\pi}{6}, \varphi = \frac{7\pi}{9}$.

To verify their claims in our scheme, we calculate the state distance of the pointer for the same expectation value and weak value of the observable $\hat{\sigma}_x$. If we assume the expectation value and weak value of $\hat{\sigma}_x$ is equal to 1, then only the $|\uparrow_x\rangle = 1/\sqrt{2}(|H\rangle + |V\rangle)$ state of $\hat{\sigma}_x$ can produce this fixed same value. After taking the related measurement procedures, we can find the final states of the SPAC state pointer for the above two cases and evaluate the distance. By following the

authors of Ref. [83], we express the distance between two states by using the Bures angle

$$D_A \equiv \arccos |\langle \Phi_{ex}|\Phi_w\rangle|, \qquad (24)$$

where $|\Phi_{ex}\rangle = D(\frac{s}{2})|\phi\rangle$ and $|\Phi_w\rangle = \mathcal{N}[2 - D(\frac{s}{2})]|\phi\rangle$ represent the final states of the SPAC state pointer caused by the same expectation value and weak value, respectively. The Bures angles [see Eq. (24)] as functions of the coupling factor s for different state parameter r are shown in Fig. 3(c). The numerical results indicate that, in our scheme, the exactly equal expectation value and weak value (i.e., $\langle \sigma_x \rangle_{ex} = \langle \sigma_x \rangle_w = 1$) have different effects on the SPAC state pointer. Here, we must mention that in our scheme the chosen corresponding state is not flexible for the same fixed eigenvalue, the expectation value, and weak value, in contrast to that in Ref. [83].

Before we jump to the next subsection related to the phase-space distribution of our measurement scheme, we want to add some analysis about the accuracy of the weak measurement based on the coherent and SPAC state pointers, respectively. In our measurement model, the general expression of the unnormalized final state of the pointer after the measurement process is given by

$$\begin{aligned}|\Psi\rangle &= \langle \psi_f | e^{-ig_0 \hat{\sigma}_x \otimes \hat{P}} | \psi_i\rangle \otimes |\Theta\rangle \\ &= \frac{\langle \psi_f | \psi_i\rangle}{2}\left[(1 + \langle \sigma_x\rangle_w)D\left(\frac{s}{2}\right) + (1 - \langle \sigma_x\rangle_w)D\left(\frac{-s}{2}\right)\right]|\Theta\rangle.\end{aligned}$$
$$(25)$$

Here $|\Theta\rangle$ is the arbitrary initial state of the pointer. Next we find the expectation values of the pointer under the final pointer state $|\Psi\rangle$ for $|\Theta\rangle$ considered as the coherent state and SPAC state, respectively.

(1) The coherent state $|\Theta\rangle = |\alpha\rangle = D(\alpha)|0\rangle$. For this pointer state, the expectation value of the position observable $\hat{X} = \sigma(\hat{a}^\dagger + \hat{a})$ after the postselected measurement is given as [59]

$$\begin{aligned}\langle X\rangle_{coh,f} &= \frac{\langle \Psi|\hat{X}|\Psi\rangle}{\langle \Psi|\Psi\rangle} \\ &= 2\sigma|\lambda|^2\{\mathrm{Re}[\alpha](1 + |\langle \sigma_x\rangle_w|^2) + s\mathrm{Re}[\langle \sigma_x\rangle_w] \\ &\quad + \mathrm{Re}[(1 - \langle \sigma_x\rangle_w^*)(1 + \langle \sigma_x\rangle_w)e^{-2is\mathrm{Im}[\alpha]}] \\ &\quad \times \mathrm{Re}[\alpha]e^{-\frac{1}{2s^2}}\},\end{aligned}$$
$$(26)$$

with

$$\begin{aligned}\lambda^{-2} &= 1 + |\langle \sigma_x\rangle_w|^2 \\ &= \mathrm{Re}[(1 - \langle \sigma_x\rangle_w^*)(1 + \langle \sigma_x\rangle_w)e^{-2is\mathrm{Im}[\alpha]}]e^{-\frac{1}{2s^2}}. \quad (27)\end{aligned}$$

In the weak measurement regime, we obtain

$$\langle X\rangle_{coh,w} = \lim_{s\to 0}\langle X\rangle_{coh,f} = g\mathrm{Re}[\langle \sigma_x\rangle_w] + \langle X\rangle_i, \qquad (28)$$

where $\langle X\rangle_i = \langle \alpha|\hat{X}|\alpha\rangle = 2\sigma\mathrm{Re}[\alpha]$ is the expectation value of $\hat{X}$ under the initial pointer state $|\alpha\rangle$. Thus, the shift of the coherent state pointer after the weak measurement is equal to

$$\delta X_{coh,w} = g\mathrm{Re}[\langle \sigma_x\rangle_w]. \qquad (29)$$

(2) The SPAC state $|\Theta\rangle = |\phi\rangle$. If we take the initial state of the pointer in the SPAC state, which we considered in

the present work, then the expectation value of the position observable $\hat{X} = \sigma(\hat{a}^\dagger + \hat{a})$ under the final pointer state $|\Phi\rangle$ [see Eq. (9)] is written as

$$\langle X\rangle_{spac,f} = \langle \Phi|\hat{X}|\Phi\rangle = 2\sigma\mathrm{Re}[\langle \hat{a}\rangle] + \langle X\rangle_{spac,i}, \qquad (30)$$

where $\langle X\rangle_{spac,i} = \langle \phi|\hat{X}|\phi\rangle = 2\sigma\gamma^2(2 + |\alpha|^2)\mathrm{Re}[\alpha]$ is the expectation value of $\hat{X}$ under the initial pointer state $|\phi\rangle$ and $\langle \hat{a}\rangle$ is given by Eq. (19). In the weak measurement regime, we obtain

$$\begin{aligned}\langle X\rangle_{spac,w} &= \lim_{s\to 0}\langle X\rangle_{spac,f} = g\mathrm{Re}[\langle \sigma_x\rangle_w] \\ &\quad - g\frac{\partial \mathrm{Var}(X)_{|\phi\rangle}}{2\sigma^2\partial\theta}\mathrm{Im}[\langle \sigma_x\rangle_w] + \langle X\rangle_{spac,i}. \quad (31)\end{aligned}$$

Here

$$\mathrm{Var}(X)_{|\phi\rangle} = \sigma^2\gamma^4(3 + 4|\alpha|^2\sin^2\theta + |\alpha|^4) \qquad (32)$$

is the variance of the position variable under the initial SPAC state $|\phi\rangle$. We can deduce that the shift of the SPAC state pointer after the weak measurement procedure is equal to

$$\begin{aligned}\delta X_{spac} &= \langle X\rangle_{spac,w} - \langle X\rangle_{spac,i} \\ &= g\mathrm{Re}[\langle \sigma_x\rangle_w] - g\frac{\partial \mathrm{Var}(X)_{|\phi\rangle}}{2\sigma^2\partial\theta}\mathrm{Im}[\langle \sigma_x\rangle_w]. \quad (33)\end{aligned}$$

We know that the SPAC state is generated by adding one photon to the coherent state [46,47]. However, we can see that, in the weak measurement procedure, the shift of the coherent state pointer only depends on the real part of the weak value $\langle \sigma_x\rangle_w$, but the shift of the SPAC state pointer is related to the real and imaginary parts of the weak value simultaneously. Equations (29) and (33) fit with Josza' s theorem [84], thus we can conclude that in the weak measurement procedure the expectation value of the system observable $\hat{X}$ of the SPAC state pointer is not exactly equal to the weak value, in contrast to the coherent state. As mentioned above, the single-photon Fock state and the coherent state correspond to the two-limit cases (for $|\alpha| \to 0$ or $|\alpha| \gg 1$) of the SPAC state. In these two extreme cases, the second term of Eq. (33) tends to zero and then the shift of the pointer is equal to the coherent state case.

B. Wigner function

To further explain the squeezing effects of the SPAC state after the postselected von Neumann measurement, in the rest of this section we study the Wigner function of $|\Phi\rangle$. The Wigner distribution function is the closest quantum analog of the classical distribution function in phase space. According to the value of the Wigner function, we can intuitively determine the strength of its quantum nature, and the negative value of the Wigner function proves the nonclassicality of the quantum state. The Wigner function exists for any state and it is defined as the two-dimensional Fourier transform of the symmetric-order characteristic function. The Wigner function for the state $\rho = |\Phi\rangle\langle \Phi|$ is written as [64]

$$W(z) \equiv \frac{1}{\pi^2}\int_{-\infty}^{+\infty}\exp(\lambda^*z - \lambda z^*)C_W(\lambda)d^2\lambda, \qquad (34)$$
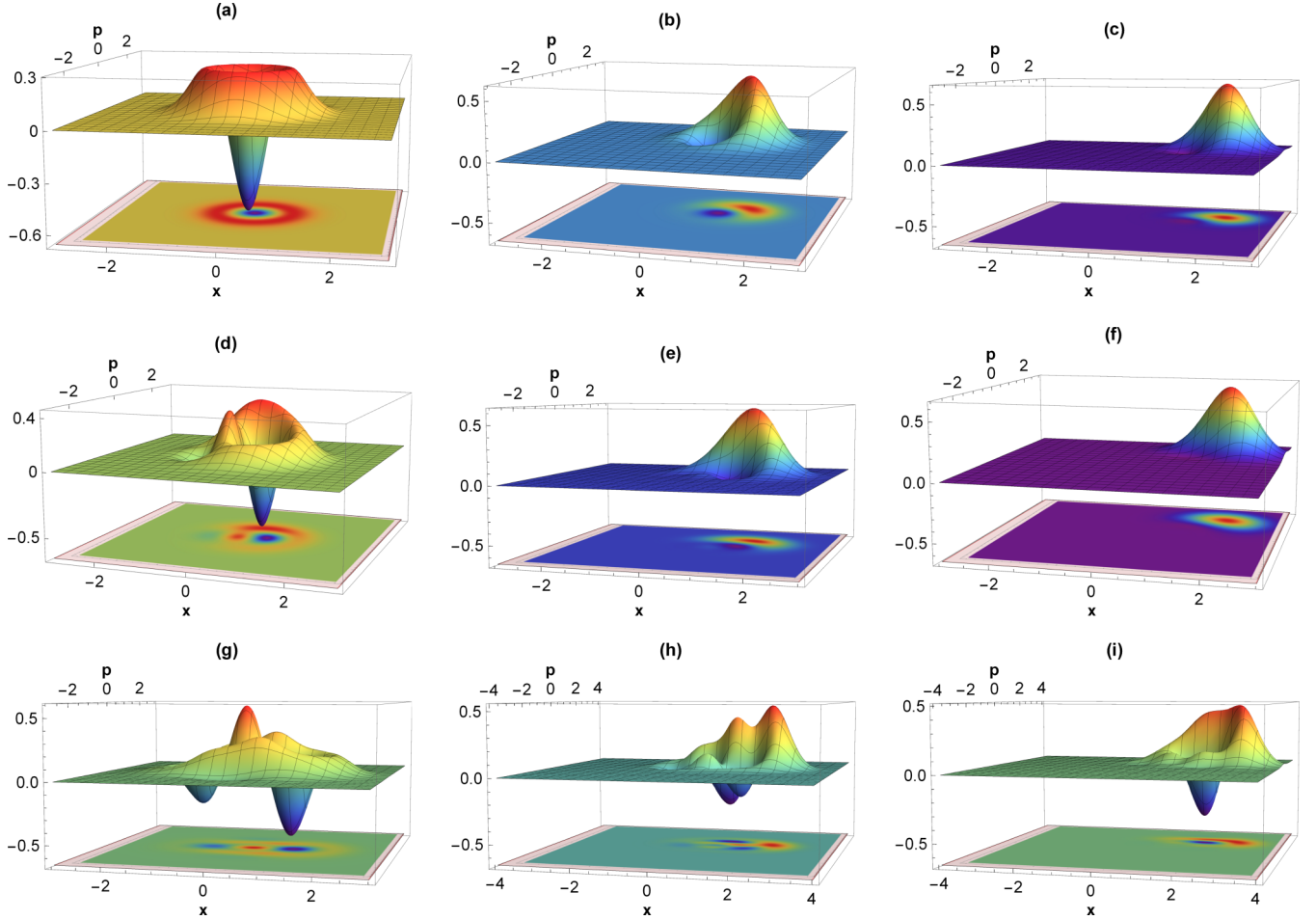
FIG. 4. Wigner function of SPAC state with changing parameters. Each column is defined for the different coherent state parameter α with $r = 0, 1, 2$, and are ordered accordingly from left to right. Panels (a) to (c) correspond to $s = 0$, (d) to (f) correspond to $s = 0.5$, and (g) to (i) correspond to $s = 2$. Other parameters are the same as those used in Fig. 3.

where $C_W(\lambda)$ is the Weyl-ordered (symmetrically ordered) characteristic function and is defined as

$$C_W(\lambda) = \mathrm{Tr}[\rho e^{\lambda a^\dagger - \lambda^* a}]. \tag{35}$$

Using the notation λ', λ'' for the real and imaginary parts of λ and setting $z = x + ip$ to emphasize the analogy between the radiation field quadratures and the normalized dimensionless position and momentum observables of the beam in phase space, we can rewrite the definition of the Wigner function in terms of x, p and λ', λ'' as

$$W(x, p) = \frac{1}{\pi^2} \int_{-\infty}^{+\infty} e^{2i(p\lambda' - x\lambda'')} C_W(\lambda) d\lambda' d\lambda''. \tag{36}$$

By substituting the final normalized pointer state $|\Phi\rangle$ into Eq. (36), we can calculate the explicit expression of its Wigner function and it reads as

$$
\begin{aligned}
W(z) ={}& \frac{2|\kappa|^2}{\pi(1 + |\alpha|^2)} e^{-2|z-\alpha|^2} \\
& \times \{|1 + \langle\sigma_x\rangle_w|^2 w(s) + |1 - \langle\sigma_x\rangle_w|^2 w(-s) \\
& + 2(-1 + |2z - \alpha|^2)\mathrm{Re}[(1 + \langle\sigma_x\rangle_w)^*(1 - \langle\sigma_x\rangle_w) \\
& \times e^{2is\mathrm{Im}[z]}]\},
\end{aligned}
\tag{37}
$$

with

$$
\begin{aligned}
w(s) ={}& e^{-\frac{1}{2}s^2} e^{-2(\mathrm{Re}[\alpha] - \mathrm{Re}[z])s} \\
& \times \left(-1 + |2z - \alpha|^2 + 2s\left[\mathrm{Re}[\alpha] - 2\mathrm{Re}[z] + \frac{s}{2}\right] \right).
\end{aligned}
\tag{38}
$$

This is a real Wigner function and its value is bounded $-\frac{2}{\pi} \leqslant W(\alpha) \leqslant \frac{2}{\pi}$ in the entirety of the phase space.

To depict the effects of the postselected von Neumann measurement on the nonclassical feature of the SPAC state, in Fig. 4 we plot its curves for different state parameters r and coupling factor s. In Fig. 4, each column from left to right, in turn, indicates the Winger functions of $|\Phi\rangle$ for different coherent state parameters r, namely $r = 0, 1$, and 2, and each row from up to down represents the different coupling factors $s = 0, 0.5$, and 2, respectively. It is observed that the positive peak of the Wigner function moves from the center to the edge position in phase space and its shape gradually becomes irregular with changing coupling factor s. From the first row [see Figs. 4(a) to 4(c)] we can see that the original SPAC state exhibits inherent features, changing from the single-photon state to coherent states, with a gradually increasing coherent state parameter r. Figures 4(d) to 4(i) indicate the phase-space

density function $W(z)$ after the postselected von Neumann measurement. Figures 4(d) to 4(f) represent the Wigner function for fixed weak interaction strength $s = 0.5$. It can be observed that the Wigner function distribution shows squeezing in phase space compared to the original SPAC state. This kind of squeezing is more pronounced with increasing coupling factor [see Figs. 4(g) to 4(i)]. Furthermore, in Figs. 4(g) to 4(i) we can see that, in the strong measurement regime, significant interference structures manifest and the negative regions became larger than the initial pointer state.

As mentioned above, the existence of progressively stronger negative regions of the Wigner function in phase space indicates the degree of nonclassicality of the associated state. From the above analysis we can conclude that, after the postselected von Neumann measurement, the phase-space distribution of the SPAC state is not only squeezed, but the nonclassicality is also more pronounced in the strong measurement regime.

V. CONCLUSION

In this paper, we studied the squeezing and Wigner function of the SPAC state after the postselected von Neumann measurement. To achieve our goal, we first determined the final state of the pointer state along with the standard measurement process. We examined the principal squeezing effects of the pointer after the postselected weak measurement procedure. We found that, in the weak measurement regime, the ordinary squeezing and AS squeezing of the SPAC state's light field increased significantly as the weak value increased.

To further explain our result, we examined the similarity between the initial SPAC state and the state after measurement. We observed that, under the weak coupling, the state after the postselected measurement maintains similarity with the initial state. However, as the intensity of the measurement increased, the similarity between them gradually decreased. This indicated that the measurement spoiled the system state if the measurement was strong. We also investigated the Wigner function of the system after postselected measurement. It was observed that, following the postselected von Neumann measurement, the phase-space distribution of the SPAC state is not only squeezed, but also develops significant interference structures in the strongly measured regime. It also possess pronounced nonclassicality characterized by a large negative area in phase space.

As previous works indicated, the higher-order squeezing, named AS squeezing, of the electromagnetic field is a natural way to generate the higher-order squeezed states [28]; it can be used for reducing the noise in the output of certain nonlinear optical devices [27,28]. We anticipate that the theoretical scheme in this paper may provide an effective method for solving practical problems in quantum information processing associated with the SPAC state.

[1] A. Mari and J. Eisert, Phys. Rev. Lett. **103**, 213603 (2009).

[2] Y. Yamamoto and H. A. Haus, Rev. Mod. Phys. **58**, 1001 (1986).

[3] H. Yuen and J. Shapiro, IEEE Trans. Inf. Theory **26**, 78 (1980).

[4] S. L. Braunstein and H. J. Kimble, Phys. Rev. Lett. **80**, 869 (1998).

[5] R. Lo Franco, G. Compagno, A. Messina, and A. Napoli, Phys. Rev. A **76**, 011804(R) (2007).

[6] R. L. Franco, G. Compagno, A. Messina, and A. Napoli, Int. J. Quantum. Inf. **07**, 155 (2009).

[7] R. L. Franco, G. Compagno, A. Messina, and A. Napoli, Open. Syst. Inf. Dyn. **13**, 463 (2006).

[8] R. Lo Franco, G. Compagno, A. Messina, and A. Napoli, Phys. Rev. A **74**, 045803 (2006).

[9] R. Lo Franco, G. Compagno, A. Messina, and A. Napoli, Eur. Phys. J-Spec. Top. **160**, 247 (2008).

[10] R. Lo Franco, G. Compagno, A. Messina, and A. Napoli, Phys. Lett. A **374**, 2235 (2010).

[11] B. R. Mollow and R. J. Glauber, Phys. Rev. **160**, 1076 (1967).

[12] R. Slusher and B. Yurke, J. Lightwave. Technol. **8**, 466 (1990).

[13] H. Yuen and J. Shapiro, IEEE Trans. Inf. Theory **24**, 657 (1978).

[14] C. M. Caves, Phys. Rev. D **23**, 1693 (1981).

[15] G. J. Milburn and S. L. Braunstein, Phys. Rev. A **60**, 937 (1999).

[16] B. Schumacher, Phys. Rev. A **54**, 2614 (1996).

[17] B. Schumacher and M. A. Nielsen, Phys. Rev. A **54**, 2629 (1996).

[18] F.-L. Li, H.-R. Li, J.-X. Zhang, and S.-Y. Zhu, Phys. Rev. A **66**, 024302 (2002).

[19] T. C. Zhang, K. W. Goh, C. W. Chou, P. Lodahl, and H. J. Kimble, Phys. Rev. A **67**, 033802 (2003).

[20] B. Kraus, K. Hammerer, G. Giedke, and J. I. Cirac, Phys. Rev. A **67**, 042314 (2003).

[21] A. Kitagawa and K. Yamamoto, Phys. Rev. A **68**, 042324 (2003).

[22] A. Dolińska, B. C. Buchler, W. P. Bowen, T. C. Ralph, and P. K. Lam, Phys. Rev. A **68**, 052308 (2003).

[23] S. L. Braunstein and H. J. Kimble, Phys. Rev. A **61**, 042302 (2000).

[24] V. Petersen, L. B. Madsen, and K. Mølmer, Phys. Rev. A **72**, 053812 (2005).

[25] J. Kempe, Phys. Rev. A **60**, 910 (1999).

[26] C. K. Hong and L. Mandel, Phys. Rev. A **32**, 974 (1985).

[27] M. Hillery, Opt. Commun. **62**, 135 (1987).

[28] M. Hillery, Phys. Rev. A **36**, 3796 (1987).

[29] C. Gerry and S. Rodrigues, Phys. Rev. A **35**, 4440 (1987).

[30] X. Yang and X. Zheng, Phys. Lett. A **138**, 409 (1989).

[31] E. K. Bashkirov and A. S. Shumovsky, Int. J. Mod. Phys. B **4**, 1579 (1990).

[32] M. H. Mahran, Phys. Rev. A **42**, 4199 (1990).

[33] P. Marian, Phys. Rev. A **44**, 3325 (1991).

[34] M. A. Mir, Int. J. Mod. Phys. B **7**, 4439 (1993).

[35] S.-D. Du and C.-D. Gong, Phys. Rev. A **48**, 2198 (1993).

[36] A. V. Chizhov, J. W. Haus, and K. C. Yeong, Phys. Rev. A **52**, 1698 (1995).

[37] R. Lynch and H. A. Mavromatis, Phys. Rev. A **52**, 55 (1995).

[38] M. A. Mir, Int. J. Mod. Phys. B **12**, 2743 (1998).

[39] R.-H. Xie and S. Yu, J. Opt. B: Quantum Semiclassical Opt. **4**, 172 (2002).

[40] R.-H. Xie and Q. Rao, Physica A **312**, 421 (2002).

[41] Z. Wu, Z. Cheng, Y. Zhang, and Z. Cheng, Physica B **390**, 250 (2007).

[42] E. K. Bashkirov, Int. J. Mod. Phys. B **21**, 145 (2007).

[43] D. K. Mishra, Opt. Commun. **283**, 3284 (2010).

[44] D. K. Mishra and V. Singh, Opt. Quantum Electron. **52**, 68 (2020).

[45] S. Kumar and D. K. Giri, J. Opt.-UK **49**, 549 (2020).

[46] G. S. Agarwal and K. Tara, Phys. Rev. A **43**, 492 (1991).

[47] A. Zavatta, S. Viciani, and M. Bellini, Science **306**, 660 (2004).

[48] A. Zavatta, S. Viciani, and M. Bellini, Phys. Rev. A **72**, 023820 (2005).

[49] P. V. P. Pinheiro and R. V. Ramos, Quantum Inf. Process. **12**, 537 (2013).

[50] Y. Wang, W.-S. Bao, H.-Z. Bao, C. Zhou, M.-S. Jiang, and H.-W. Li, Phys. Lett. A **381**, 1393 (2017).

[51] M. Miranda and D. Mundarain, Quantum Inf. Process. **16**, 298 (2017).

[52] S. Srikara, K. Thapliyal, and A. Pathak, Quantum Inf. Process. **19**, 371 (2020).

[53] J.-R. Zhu, C.-Y. Wang, K. Liu, C.-M. Zhang, and Q. Wang, Quantum Inf. Process. **17**, 294 (2018).

[54] J.-J. Chen, C.-H. Zhang, J.-M. Chen, C.-M. Zhang, and Q. Wang, Quantum Inf. Process. **19**, 198 (2020).

[55] Y. Aharonov, D. Z. Albert, and L. Vaidman, Phys. Rev. Lett. **60**, 1351 (1988).

[56] K. Nakamura, A. Nishizawa, and M.-K. Fujimoto, Phys. Rev. A **85**, 012113 (2012).

[57] B. de Lima Bernardo, S. Azevedo, and A. Rosas, Opt. Commun. **331**, 194 (2014).

[58] Y. Turek, H. Kobayashi, T. Akutsu, C.-P. Sun, and Y. Shikano, New. J. Phys. **17**, 083029 (2015).

[59] Y. Turek, W. Maimaiti, Y. Shikano, C.-P. Sun, and M. Al-Amri, Phys. Rev. A **92**, 022109 (2015).

[60] Y. Turek and T. Yusufu, Eur. Phys. J. D **72**, 202 (2018).

[61] Y. Turek, Chin. Phys. B **29**, 090302 (2020).

[62] Y. Turek, Eur. Phys. J. Plus **136**, 221 (2021).

[63] A. Luks, V. Perinova, and J. Perina, Opt. Commun. **67**, 149 (1988).

[64] G. Agarwal, *Quantum Optics* (Cambridge University Press, Cambridge, England, 2013).

[65] J. von Neumann, *Mathematical Foundations of Quantum Mechanics* (Princeton University Press, Princeton, NJ, 1955).

[66] Y. Aharonov and A. Botero, Phys. Rev. A **72**, 052111 (2005).

[67] A. Di Lorenzo and J. C. Egues, Phys. Rev. A **77**, 042108 (2008).

[68] A. K. Pan and A. Matzkin, Phys. Rev. A **85**, 022122 (2012).

[69] O. Hosten and P. Kwiat, Science **319**, 787 (2008).

[70] L. Zhou, Y. Turek, C. P. Sun, and F. Nori, Phys. Rev. A **88**, 053815 (2013).

[71] M. Pfeifer and P. Fischer, Opt. Express **19**, 16508 (2011).

[72] P. B. Dixon, D. J. Starling, A. N. Jordan, and J. C. Howell, Phys. Rev. Lett. **102**, 173601 (2009).

[73] D. J. Starling, P. B. Dixon, A. N. Jordan, and J. C. Howell, Phys. Rev. A **80**, 041803(R) (2009).

[74] D. J. Starling, P. B. Dixon, A. N. Jordan, and J. C. Howell, Phys. Rev. A **82**, 063822 (2010).

[75] O. S. Magaña-Loaiza, M. Mirhosseini, B. Rodenburg, and R. W. Boyd, Phys. Rev. Lett. **112**, 200401 (2014).

[76] G. I. Viza, J. Martínez-Rincón, G. A. Howland, H. Frostig, I. Shomroni, B. Dayan, and J. C. Howell, Opt. Lett. **38**, 2949 (2013).

[77] P. Egan and J. A. Stone, Opt. Lett. **37**, 4991 (2012).

[78] A. G. Kofman, S. Ashhab, and F. Nori, Phys. Rep. **520**, 43 (2012).

[79] J. Dressel, M. Malik, F. M. Miatto, A. N. Jordan, and R. W. Boyd, Rev. Mod. Phys. **86**, 307 (2014).

[80] P. Shukla and R. Prakash, Mod. Phys. Lett. B **27**, 1350086 (2013).

[81] Y. Pan, J. Zhang, E. Cohen, C.-W. Wu, P.-X. Chen, and N. Davidson, Nat. Phys. **16**, 1206 (2020).

[82] K. Araya-Sossa and M. Orszag, Phys. Rev. A **103**, 052215 (2021).

[83] L. Vaidman, A. Ben-Israel, J. Dziewior, L. Knips, M. Weißl, J. Meinecke, C. Schwemmer, R. Ber, and H. Weinfurter, Phys. Rev. A **96**, 032114 (2017).

[84] R. Jozsa, Phys. Rev. A **76**, 044103 (2007).